Electronic Supplementary Material (ESI) for Nanoscale.
This journal is © The Royal Society of Chemistry 2018

Supporting Information

Polymers Mediate One-Pot Route for Functionalized Quantum Dot Barcodes with a Large Encoding Capacity

Ding Sheng-zi Zhang[a], *Yang Jiang*[a], *Dan Wei*[a], *Xunbin Wei*[a], *Hong Xu*[*a], *Hongchen Gu*[*a]

[a] Shanghai Jiao Tong University Affiliated 6th Hospital, School of Biomedical Engineering, Shanghai Jiao Tong University, Shanghai 200030, P. R. China

E-mail: xuhong@sjtu.edu.cn, hcgu@sjtu.edu.cn

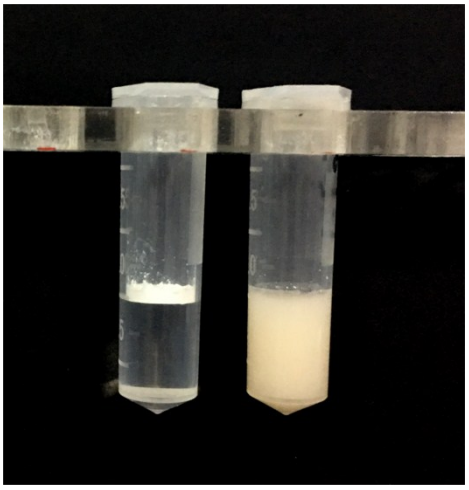

Fig. S1 Photographs of MPS (left) and QDs@MPS-PSMA (right) dispersed in water under natural light.

Fig. S1 shows the MPS are floating on the surface of water, whereas the QDs@MPS-PSMA are well dispersed in water. This implies that the hydrophobic MPS are successfully transformed into hydrophilic QDs@MPS-PSMA via the one-pot PSMA-mediated method.

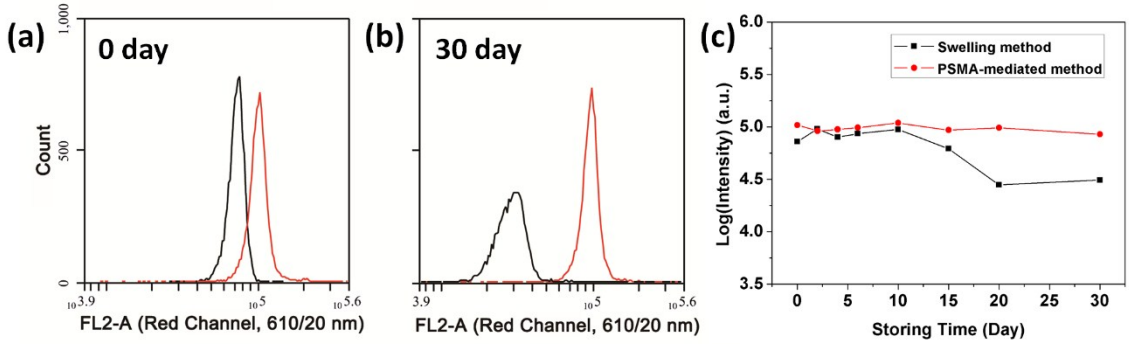

Fig. S2 (a) Fluorescence histograms of QD-doped beads prepared using the PSMA-mediated method (red line) and the traditional swelling method (black line) at the beginning of storage. (b) Fluorescence histograms of QD-doped beads prepared using the PSMA-mediated method (red line) and the traditional swelling method (black line) after 30 days of storage. (c) The photostability of the QD-doped beads when stored in DI water for one month. The corresponding fluorescence intensity is measured by flow cytometer.

Table S1 Fluorescence intensity of QD-doped beads prepared with different methods[a)]

QD-doped beads	Int. at 1st day	Int. at 30th day
Beads from PSMA-mediated method	104173.69	98261.27
Beads from solvent-driven trapping method	72456.01	31169.09

a) The intensity of beads is detected with flow cytometer at FL2 channel.

Data in **Fig. S2** and **Table S1** shows that when we set the same amount of QDs and MPS, we could obtain stronger and more stable fluorescence intensity of QD-doped beads if we utilize PSMA-mediated method. It suggests that our method could prepare QD barcodes with greater fluorescence performance than solvent-driven trapping method.

Table S2 Absolute quantum yield of QDs at different environment during the preparation

QDs at different environment	QDs/$CHCl_3$	QDs@MPS-PSMA in chloroform	QDs@MPS-PSMA in water	QDs/PSMA micelles in water
Quantum yield	77.5%	60.2%	45.7%	66.4%

The results (see **Table S2**) shows that the PL QY of QDs@MPS in chloroform is less than that of QDs/$CHCl_3$. There are two kinds of QDs in the sample of QDs@MPS in chloroform: one is QDs dispersed in chloroform, another is QDs entrapped inside the polystyrene beads. The determined QY is the overall QY of the sample, which includes the two different kinds of QDs as well as the absorption or scattering effect from the polystyrene beads. So the final QY of QDs@MPS in chloroform is different from the original one.

For the final product QDs@MPS-PSMA in water, their QY is lower than the QDs/$CHCl_3$ while QDs/PSMA micelles in water is a bit higher. The main reason that could account for this phenomena is that during the process of phase transformation, alkaline water may have a bit damage to the ligands on the surface of QDs, which would induce the slight decrease of the QY of entrapped QDs.[1,2]

For the comparatively higher QY of QDs/PSMA micelles in water, we think it is the interference of scattering effect from MPS that cause the different QYs between QDs@MPS-PSMA in water and QDs/PSMA micelles in water.

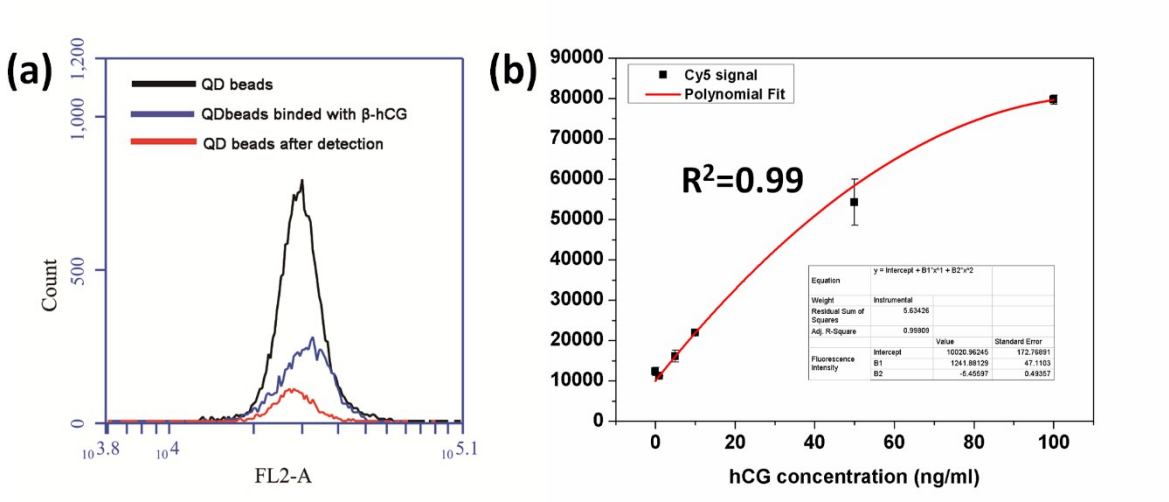

Fig. S3 Fluorescence histogram of QDs@MPS-PSMA at different environments. Black peak represents original QDs@MPS-PSMA, blue peak represents QDs@MPS-PSMA after conjugating with anti β-hCG antibody, red peak represents QDs@MPS-PSMA immunocomplex after sandwich immunoassay. (b) Sensitivity plots of immunoassays for hCG detection.

Fig. S3-a proves that QDs@MPS-PSMA has excellent photo-stability, which could meet the multiplex-detection requirements. The well-fitting of sensitivity plots and polynomial equation with R^2=0.99 suggests that QD@MPS-PSMA is potential to be used as barcodes for multiplex detection.

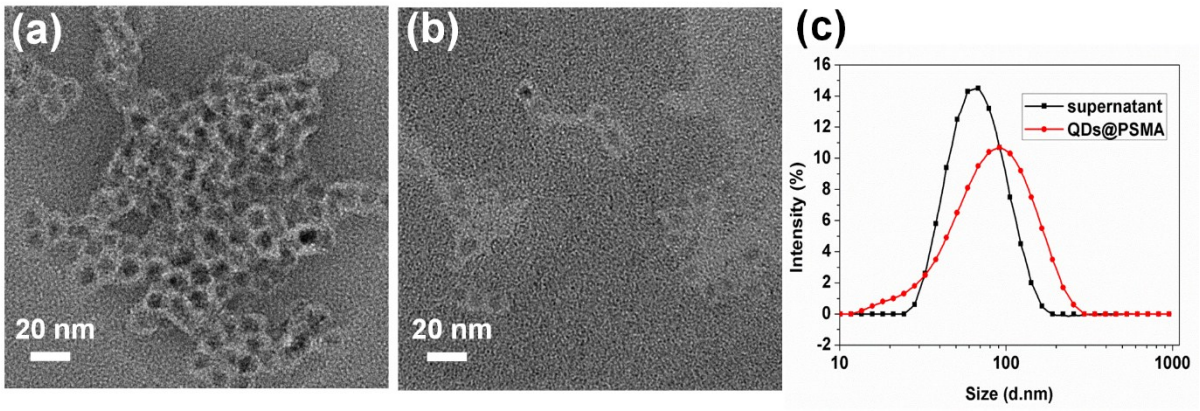

Fig. S4 (a) TEM characterization of QD/PSMA aggregations dispersed in the supernatant of the reaction liquid during the preparation of beads using the PSMA-mediated method. (b) TEM characterization of QD/PSMA micelles prepared through emulsification process. (c) Hydrodynamic diameters of the QD/PSMA aggregations and QD/PSMA micelles separately from (a) and (b) determined by DLS.

Table S3 Hydrodiameter and Zeta potential of QD/PSMA assembly

QD/PSMA assembly	Zeta (mV)	Size (nm)	PDI
QD/PSMA aggregations in reaction supernatant	-39.85 ± 4.17	64.22 ± 0.17	0.194 ± 0.006
QD/PSMA micelles[3]	-35.95 ± 5.02	66.53 ± 1.06	0.283 ± 0.007

Table S3 shows that the QD/PSMA aggregations in reaction supernatant has similar size and surface zeta potential with the QD/PSMA micelles directly prepared according to Colvin's work.[3]

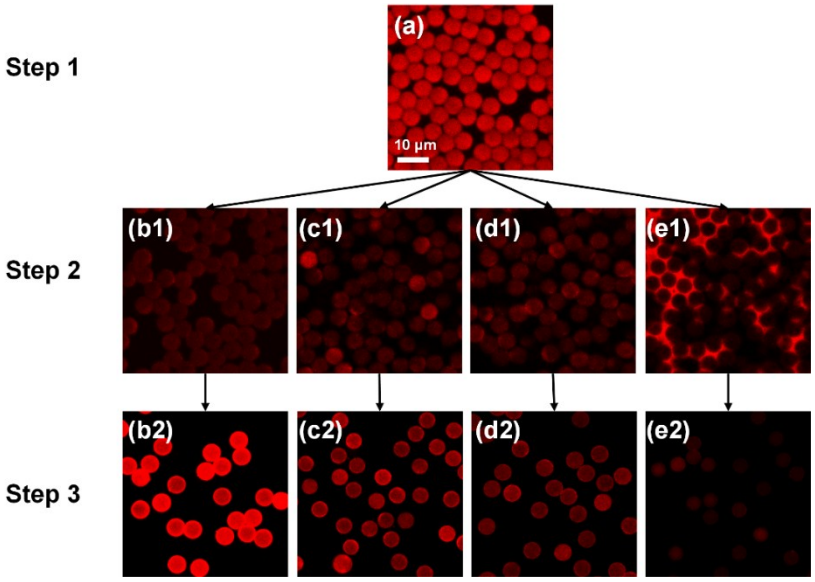

Fig. S5 Confocal images of mesoporous beads at different steps during the preparation of QDs@MPS-PSMA. (a) 35 μg of QDs were mixed with 1.37 mg of MPS in chloroform for 10 min at step 1. (b1)-(e1) PSMA was added into QDs/MPS/chloroform mixture from (a) at different mass ratios of PSMA/MPS (0.03, 0.15, 0.3, and 1.17) and mixed for another 5 min at step 2. (b2)-(e2) After the alkaline solution with the same volume was injected into QD/PSMA/MPS/chloroform mixtures from (b1) to (e1), separately at step 3.

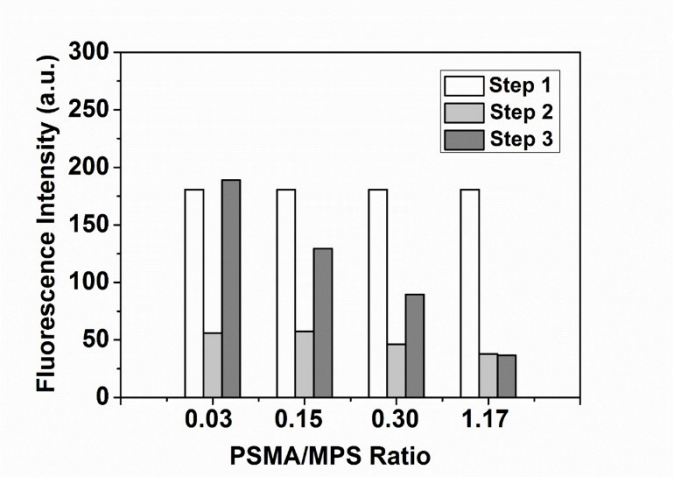

Fig. S6 Fluorescence intensity of QDs@MPS-PSMA at three steps during the preparation when PSMA/MPS ratios are different.

As shown in **Fig. S5**, fluorescence intensity of the beads decreased dramatically after the PSMA molecules were introduced into the mixture. To be specific, the quantitative data in **Fig. S6** shows that when PSMA/MPS ratio is gradually increased from 0.03 to 1.17, the remaining ratio of bead intensities decreases from 30% to 20% correspondingly at step 2 but recovers to different extents at step 3.

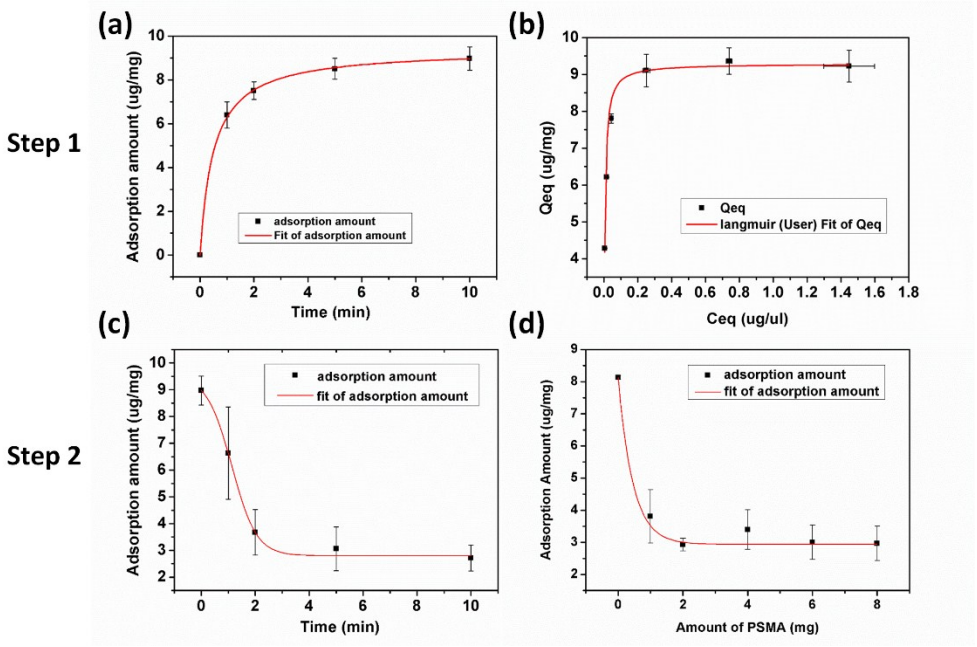

Fig. S7 (a) Adsorption kinetics of QDs to MPS in chloroform at step 1. (b) Adsorption thermodynamics of QDs to MPS in chloroform at step 1. (c) Desorption kinetics of QDs to MPS in chloroform after PSMA addition at step 2 (PSMA/MPS mass ratio is 0.3). (d) Desorption thermodynamics of QDs to MPS in chloroform after PSMA addition at step 2.

Fig. S7-a depicted a kinetical process of QDs adsorption, showing that after 10 min, the adsorption/desorption process of QDs came to an equilibrium and the adsorption amount of QDs became stable. **Fig. S7-b** depicted QDs adsorption isotherm and we also produced an equation (1-1) below, which is well fitted with Langmuir isotherm model with R-square of 0.999. Thereforem we concluded that the process of QDs adsorbing into MPS perfectly conforms to the Langmuir monolayer adsorption.

$$Q_e = C_{max} \times \frac{bx}{1+bx} \qquad (1\text{-}1)$$

In equation (1-1), $C_{max} = 9.294$, $b = 190.544$

Fig. S7-c and **Fig. S7-d** separately depicted the kinetical and thermodynamical process of QDs after the injection of PSMA molecules. The results showed that once PSMA molecules were injected, the adsorption amount of QDs would declined quickly, indicating that the

PSMA and QDs may strongly interact in chloroform, which induces desorption of the QDs from the beads.

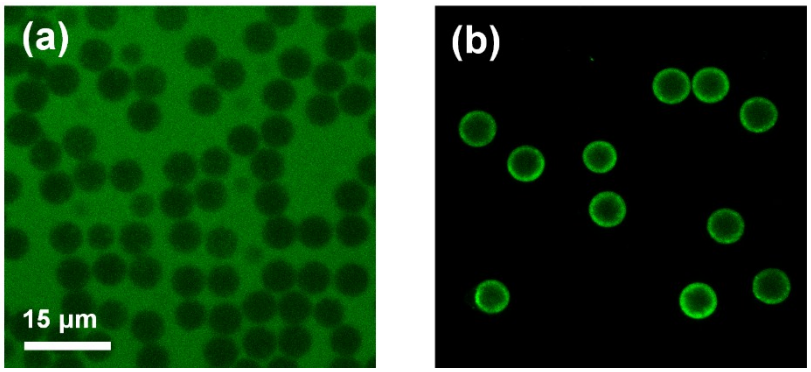

Fig. S8 (a) Confocal image of MPS after 5-AF labelled PSMA were mixed with MPS for 10 min. (b) Confocal image of QD-doped beads prepared with the PSMA-mediated method when the original concentration of QDs was set for 0 mg/ml. the beads were observed at Channel 1 (500-530 nm); the laser excitation wavelength was 488 nm.

Fig. S8-a shows that most 5-AF-labelled PSMA are dissolved in chloroform rather than being located at the interior of the mesoporous beads, which means that PSMA molecules have stronger interaction with chloroform instead of MPS.

For the fluorescent beads in **Fig. S8-b**, the fluorescence distribution of PSMA is similar to that of QDs in QDs@MPS-PSMA, suggesting that the presence of QDs almost has no effect on the behavior of the PSMA, and it is the PSMA molecules that determine the encapsulation and distribution of QDs during the QD-loading process.

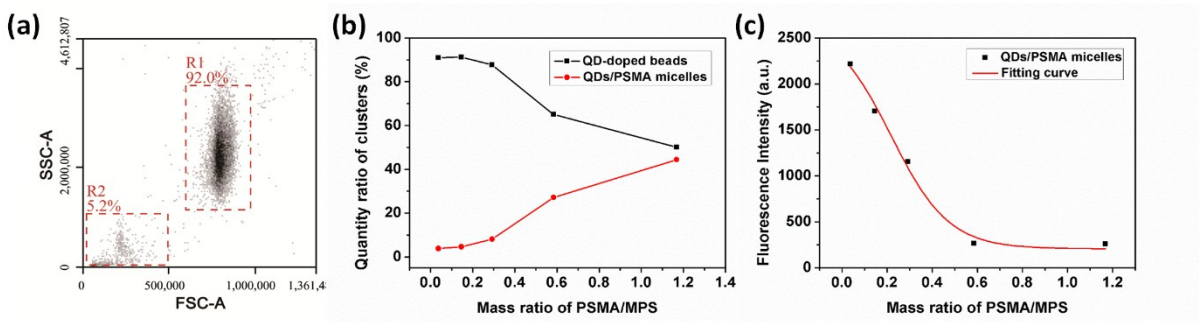

Fig. S9 (a) Scattering plot of QD-doped beads obtained via flow cytometry. R1 region represents the distribution of QD-doped beads and R2 region represents the distribution of QD/PSMA micelles. (b) Quantity percentage of QD-doped beads (black line) and QD/PSMA micelles measured by flow cytometry versus the mass ratio of PSMA/MPS.[3,4] (b) Fluorescence intensity of the QD/PSMA micelles measured by flow cytometry versus the mass ratio of PSMA/MPS.

As **Fig. S9-b** shown, with the increase of mass ratio of PSMA/MPS, the percentage of QD-doped beads (R1 region) is decreased and the percentage of QD/PSMA micelles (R2 region) is increased, suggesting that the increased PSMA amount would lead to the increased desorption of QD/PSMA micelles from the porous walls. Additionally, QD/PSMA micelles have fluorescence intensities (**Fig. S9-c**) because of the existence of QDs. With the increase of mass ratio of PSMA/MPS, the fluorescence intensity of QD/PSMA micelles is gradually decreasing. It is possible that when PSMA is less, several QDs would aggregate and forming big QD/PSMA micelles with comparatively high fluorescence intensity. When PSMA is adequate, QD/PSMA micelles would only have one QD encapsulated inside PSMA, resulting in low fluorescence intensity. When PSMA continues increasing, the fluorescence intensity of QD/PSMA micelles become stable. The phenomena observed above well conform to the mechanism proposed in Fig. 6g.

References

1 J. Zylstra, J. Amey, N. J. Miska, L. S. Pang, C. R. Hine, J. Langer, R. P. Doyle and M. M. Maye, *Langmuir*, 2011, **27**, 4371–4379.

2 A. Prakash, H. Zhu, C. J. Jones, D. N. Benoit, A. Z. Ellsworth, E. L. Bryant and V. L. Colvin, *ACS Nano*, 2009, **3**, 2139–2146.

3 W. W. Yu, E. Chang, J. C. Falkner, J. Zhang, a M. Al-Somali, C. M. Sayes, J. Johns, R. Drezek and V. L. Colvin, *J. Am. Chem. Soc.*, 2007, 129, 2871–2879.

4 E. E. Lees, T. Nguyen, A. H. a. Clayton, P. Mulvaney, B. W. Muir and P. Mulvaney, *ACS Nano*, 2009, 3, 1121–8.